energy&fuels

Article

pubs.acs.org/EF

Hydrocarbon Synthesis from Carbon Dioxide and Hydrogen: A Two-Step Process

David M. Drab,[†] Heather D. Willauer,*[,†] Matthew T. Olsen,[†] Ramagopal Ananth,[‡] George W. Mushrush,[†] Jeffrey W. Baldwin,[§] Dennis R. Hardy,[∥] and Frederick W. Williams[⊥]

[†]Materials Science and Technology Division, Code 6300.2, [‡]Chemistry Division, Code 6185, [§]Acoustics Division, Code 7136, and [⊥]Chemistry Division, Code 6104, United States Naval Research Laboratory, 4555 Overlook Avenue Southwest, Washington, District of Columbia 20375, United States

[∥]Nova Research, Incorporated, 1900 Elkin Street, Alexandria, Virginia 22308, United States

ABSTRACT: CO_2 hydrogenation to olefins and ethylene oligomerization were investigated in efforts to improve catalyst composition and reaction conditions needed for scale-up. The hydrogenation of CO_2 to hydrocarbons is investigated over γ-alumina-supported iron-based catalysts modified with manganese and potassium promoters and a silica-stabilized coating under fixed-bed reactor conditions to produce unsaturated hydrocarbons as feedstock chemicals for jet fuel synthesis. The stabilizer is introduced by impregnating the K/Mn/Fe on Al_2O_3 catalyst with tetraethylorthosilicate (TEOS) to minimize the deactivating effects of water on catalyst activity in CO_2 hydrogenation. The K/Mn/Fe on Al_2O_3 catalyst modified with the TEOS and reduced in CO produced a lighter end fraction of olefins compared to the catalyst reduced in H_2. To increase the chain length of the olefins formed in the CO_2 hydrogenation step, investigation of the oligomerization reaction is conducted in a separate experiment, where pure ethylene is used as a model olefin. Ethylene oligomerization over pelletized amorphous silica−alumina (ASA)-supported Ni catalysts demonstrated high conversion and selectivity toward the jet fuel fraction (C_8−C_{16}) at a very low mass hourly space velocity (MHSV).

1. INTRODUCTION

As petroleum-derived fuels continue to dramatically increase in price and worldwide future availability is in question, this scenario presents scientists with a unique challenge and an opportunity to develop new technologies to meet current and future energy demands.[1] These future technologies must minimize their impact on the environment, specifically carbon dioxide (CO_2) emissions.[1] Because CO_2 is readily available from the air, seawater, and as a byproduct of many industrial energy-producing processes that include gas-, oil-, and coal-fired power plants and conventional Fischer−Tropsch (FT) processes, it could serve as an abundant chemical feedstock for the production of energy-rich hydrocarbons similar to middle-distillate fuels.[1] Additionally, processes that use waste CO_2 from the environment could be envisioned as CO_2-neutral.[2]

The U.S. Naval Research Laboratory (NRL) has recently reported developing a process to recover CO_2 from seawater.[3−6] CO_2 is 140 times more concentrated in seawater than in air on a weight per volume basis (g/mL).[2] Because this technology is currently being scaled and optimized, new and improved catalysts are being developed for the conversion of CO_2 to energy-rich hydrocarbons by NRL[7−10] and others.[11−17] The current research of NRL involves a two-step synthetic approach for producing liquid hydrocarbons from CO_2 and hydrogen (H_2).

In the first-step, CO_2 and H_2 are reacted over an iron-based catalyst to produce light olefins. The mechanism of CO_2 hydrogenation has been proposed to occur in two steps, as shown in eqs 1 and 2.[9,11] The reverse water-gas shift (RWGS, eq 1 below) is endothermic and produces carbon monoxide (CO). This CO is then carried forward in an exothermic FT synthesis step (eq 2), producing predominantly monounsaturated hydrocarbons (eq 3). Carbon dioxide is also hydrogenated directly to methane, in a widely cited thermodynamically favorable and highly competitive side reaction (eq 4).

$$nCO_2 + nH_2 \rightleftarrows nCO + nH_2O \quad (1)$$

$$nCO + 2nH_2 \rightarrow (CH_2)_n + nH_2O \quad (2)$$

$$nCO_2 + 3nH_2 \rightarrow (CH_2)_n + 2nH_2O \quad (3)$$

$$CO_2 + 4H_2 \rightarrow CH_4 + 2H_2O \quad (4)$$

The water formed in the primary reactions involved in CO_2 hydrogenation (eqs 1−4) and typical FT synthesis is known to negatively influence catalyst activity and product selectivity.[18−20]

One objective of this study is to modify the catalyst surface with a silica-stabilized coating to prevent the water vapor produced in the reaction sequence (eqs 1 and 2) from negatively influencing catalyst activity by reoxidation or accelerated crystallization of the metal oxide surface.[21] By decreasing the effects of water vapor on the catalyst surface, the equilibrium at the catalyst surface should favorably shift to the production of desired intermediates such as olefins over intermediates such as CO or methane (eqs 1−3). Light olefins (C_2−C_6) produced from the reaction of CO_2 and H_2 may be

Special Issue: Ultraclean Fuels Production and Utilization

Received: June 13, 2013
Revised: August 12, 2013
Published: August 14, 2013

dx.doi.org/10.1021/ef4011115 | *Energy Fuels* 2013, 27, 6348−6354

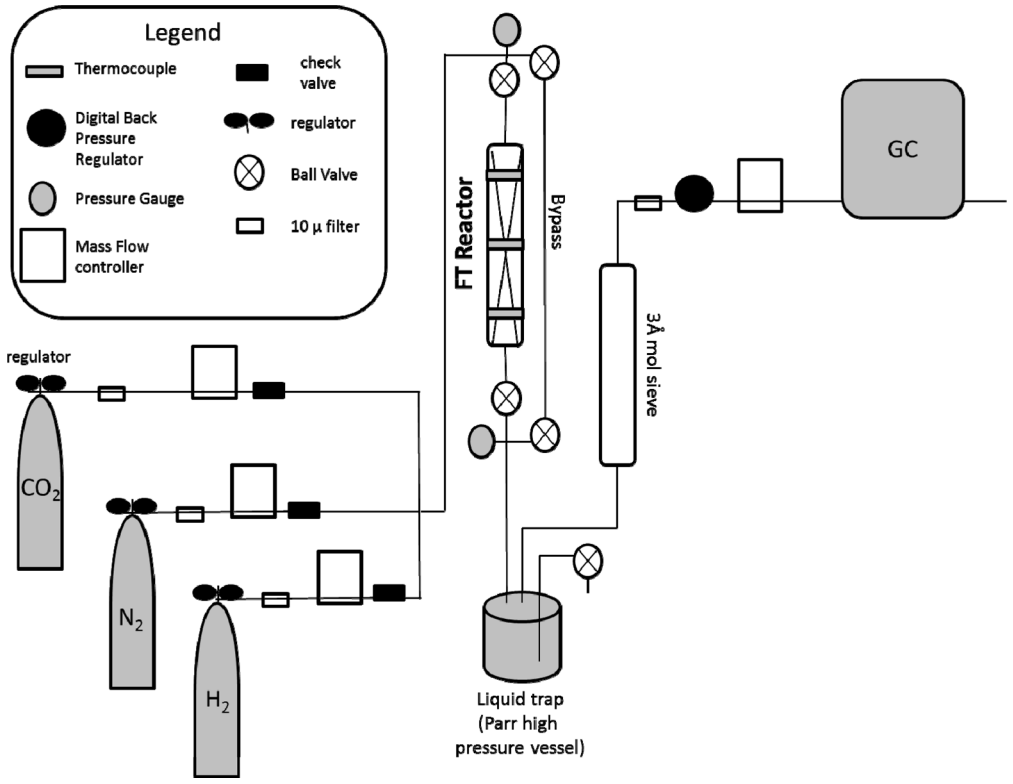

Figure 1. Reactor dimensions [9 in. (22.86 cm) length, 0.5 in. (1.27 cm) outer diameter, 0.375 in. (0.9525 cm) inner diameter, 0.994 in.^{3} (65.16 cm^3 volume)]; 17.82 g of Fe/Mn/K alumina catalyst with 2.18 g of inert material; temperature, 300 °C; flow (H_2), 75 sccm; flow (CO_2), 25 sccm; flow (N_2), 10 sccm; and pressure, 265 psig.

further reacted in a second, sequential reactor by oligomerizing to higher linear olefins.[22−24] The low-temperature oligomerization of ethylene over Ni-exchanged amorphous silica−alumina (ASA) has been reported extensively by Heveling et al.[25−27] and others,[28,29] where the reaction generates a product distribution selective for even-numbered carbon oligomers (C_4−C_{22}).[30] As part of a second objective, data from the oligomerization of pure ethylene are reported as a model olefin for the development of new and improved ASA-supported nickel catalysts for the direct and selective oligomerization to higher molecular weight olefins in the second step of a two-step approach for producing liquid hydrocarbons from carbon dioxide and hydrogen. These higher hydrocarbons can be direct substitutes for crude-oil-distilled middle-distillate fuels.

2. EXPERIMENTAL SECTION

2.1. Chemicals and Materials. Chemicals were reagent-grade and were obtained from Aldrich Chemical Co., Milwaukee, WI, and, unless noted otherwise, were used as received.

2.2. Catalyst Preparation. *2.2.1. K/Mn/Fe on Al_2O_3 Catalyst.* K/Mn/Fe on the γ-Al_2O_3 catalyst was prepared by the incipient wetness impregnation (IWI) method, where $Fe(NO_3)_3{\cdot}9H_2O$ (327.7 g), $KMnO_4$ (92.2 g), and KNO_3 (13.9 g) were dissolved in boiling deionized water (0.5 L) and slowly poured over γ-Al_2O_3 (389.5 g, Matheson Coleman and Bell, surface area of 218.3 m^2/g, pore radius of 1.2−3.7 nm, and 80−200 mesh) until excess liquid was just observed, at which point the remaining metal salt solution was added. The mixture was slowly dried on a hot plate (80−90 °C) with frequent stirring until achieving a tacky dryness and then calcinated at 350 °C in a furnace for 87 h in air. Caution! Make sure to prepare the mixture in a well-ventilated hood because a large volume of NO_2 gas is released in the process. The resulting dark maroon powder was collected and gently ground to remove visible clumps (yield = 506.4 g). A portion of the above K/Mn/Fe on Al_2O_3 catalyst was further functionalized with a silica layer by a method reported in the literature,[21] where K/Mn/Fe on Al_2O_3 was impregnated with 9% weight silica by adding tetraethylorthosilicate (TEOS) in hexane with stirring at room temperature. The catalyst is then dried overnight prior to heating at 120 °C in static air for 2 h. The final silica-coated K/Mn/Fe on Al_2O_3 was obtained by calcinating the sample at 540 °C for 4 h.

2.2.2. ASA Particles. All ASA pellets were prepared by co-precipitating silica from TEOS and alumina from $Al(NO_3)_3{\cdot}9H_2O$ to target a 5 or 15% Al content by base-catalyzed hydrolysis using concentrated NH_4OH (28%) by titration. Hydrogels at specified pH values were obtained on the basis of a modified literature procedure[18] by monitoring the titration progress with a pH probe (Orion 4-Star pH-ISE Benchtop pH meter with Ross Ultra Rugged pH probe, 8104BNUWP) and then aging for 1 h at 45 °C. The obtained hydrogel was then filtered and washed with deionized water prior to spreading the formed hydrogels onto perforated stainless-steel sheets (grade 304, hole diameter of 0.045 in. and hole depth of 0.0178 in.). Upon baking in an oven at 110 °C for 1 h, the ASA particles were obtained as small, white pellets.

2.2.3. Ni-Exchanged Amorphous Silica−Alumina (NiASA). The above ASA materials were further exchanged with nickel cations by an ion-exchange protocol reported elsewhere.[31] Each ASA sample was combined in a round-bottom flask with a 1 M solution of $Ni(NO_3)_2{\cdot}6H_2O$ in absolute ethanol (80 mL of Ni solution per 6 g of ASA). While gently tumbling on a rotary evaporator at atmospheric pressure heated by an oil bath, each ASA sample was refluxed in the nickel solution for 4 h prior to filtering and washing the particles several times with deionized water. The final NiASA particles were isolated and dried in an oven at 110 °C.

2.2.4. Calcinated ASA (ASAcal) and Ni-Exchanged Calcinated ASA (NiASAcal). Samples of the prepared ASA were calcinated under static air in a furnace set to 550 °C for 1 h. Samples of calcinated ASA were exchanged with nickel cation following the same NiASA preparation described above. Additionally, a commercial ASA (Sigma-Aldrich, grade 135) was also used as a catalyst support,

dx.doi.org/10.1021/ef4011115 | Energy Fuels 2013, 27, 6348−6354

Table 1. Product Selectivity (%, Carbon Based), Olefin/Paraffin Ratio, CO_2 Conversion, and ASF Values over K/Mn/Fe Catalysts Impregnated on Al_2O_3 and Reduced in CO under Fixed-Bed Conditions

		selectivity (%, carbon based)										
time (h)	CO_2 conversion (%)	CO (%)	C_1 (%)	C_2 (%)	C_3 (%)	C_4 (%)	C_5 (%)	C_6 (%)	C_2–C_{6+}	C_2–C_{6+} yield (%)	olefin/paraffin	α C_1–C_{6+}
12	40.7	9.6	33.9	19.6	20.6	13.8	2.4	0.0	56.4	23.0	4.1	0.38
24	31.0	12.1	27.8	17.3	18.6	13.0	11.0	0.1	59.9	18.6	5.2	0.30
36	31.0	11.6	25.7	16.5	17.9	12.4	9.0	6.8	62.6	19.4	5.3	0.53
48	35.1	10.6	25.2	16.4	18.0	12.5	9.1	8.0	64.0	22.5	5.3	0.54
116	33.4	11.0	23.5	16.3	17.9	12.4	9.0	9.8	65.4	21.8	5.3	0.56

Table 2. Product Selectivity (%, Carbon Based), Olefin/Paraffin Ratio, CO_2 Conversion, and ASF Values over K/Mn/Fe Catalysts Impregnated on Al_2O_3 and Reduced in CO under Fixed-Bed Conditions: Catalyst Modified with TEOS

		selectivity (%, carbon based)										
time (h)	CO_2 conversion (%)	CO (%)	C_1 (%)	C_2 (%)	C_3 (%)	C_4 (%)	C_5 (%)	C_6 (%)	C_2–C_{6+}	C_2–C_{6+} yield (%)	olefin/paraffin	α C_1–C_{6+}
12	38.8	11.2	35.5	17.8	20.4	14.0	1.1	0	53.3	20.7	2.6	0.32
24	30.2	15.8	29.3	15.2	17.3	12.4	9.6	0.4	54.9	16.6	3.4	0.35
36	29.2	16.4	27.6	14.6	16.6	11.8	9.1	3.9	56.0	16.3	3.6	0.49
48	29.2	16.8	26.7	14.3	16.2	11.3	8.4	6.5	56.7	16.6	3.7	0.52
60	29.2	16.9	26.1	14.2	16.1	11.2	8.2	7.4	57.1	16.7	3.7	0.59
72	29.2	16.7	25.9	14.2	16.1	11.2	8.2	7.7	57.4	16.8	3.8	0.59
90	31.3	15.7	25.9	14.4	16.2	11.0	8.0	8.7	58.2	18.2	3.8	0.60

where Ni exchange and calcination procedures are similar to those described above.

2.3. Material Characterization. Material properties of all ASA and NiASA (calcinated and uncalcinated) were characterized by X-ray photoelectron spectroscopy (XPS), microporosity measurement, field emission scanning electron microscopy (FESEM), and Fourier transform infrared (FTIR) spectroscopy. XPS was used to assess the surface species and quantities present on the different ASA particles as well as commercial ASA using a K-Alpha instrument (Thermo Scientific, U.K.) with an instrument-specific powder sample holder and Unifit (version 2011, revision F) software for data analysis. A monochromated Al Kα X-ray source was used, where the excitation energy was 1486.68 ± 0.2 eV and the dwell time (0.05 s) and pass energy (200 eV) were also held constant. The binding energy (BE) range was viewed from −9.92 to +1350.08 eV, for a total of 1361 data points per analysis. Structural and chemical characterizations were performed with FESEM (model LEO DSM 982, LEO) operated at an accelerating voltage between 5 and 10 kV, and the working distance varied from 8 to 12 mm.

Brunauer–Emmett–Teller (BET) surface areas were measured using a Micrometrics ASAP2010 accelerated surface area and porosimetry system. FTIR spectra were recorded for samples pressed in KBr pellets (1:100 sample/KBr weight ratio) and analyzed using OMNIC software (Thermo Electron Corporation, 2001) over the frequency range of 4000–400 cm^{-1}. Ni-exchanged ASA samples were submitted for elemental analysis, where the percent Ni concentration was determined by inductively coupled plasma atomic emission spectroscopy (ICP–OES) analysis (Galbraith Laboratories, Inc., Knoxville, TN).

2.4. Carbon Dioxide Hydrogenation. A fixed-bed reactor (Figure 1) was prepared by loading a mixture of the K/Mn/Fe on γ-Al_2O_3 catalyst and γ-Al_2O_3 filler (17.82 g of catalyst and 2.18 g of alumina for 20.00 g total) in a stainless-steel tube (9 in. long, $^1/_2$ in. outer diameter, and $^3/_8$ in. inner diameter), drying with nitrogen [100 standard cubic centimeters per minute (sccm), 265 psig, and 300 °C], and finally reducing the catalyst with CO or H_2 (2 h, 300 °C, and 100 sccm). Once reduced, the reactor was purged with nitrogen for 1 h prior to introducing the reactive gases, where flows were set by mass flow controllers (Sierra Instruments) at 100 sccm (25 sccm CO_2 and 75 sccm H_2), with 10 sccm of nitrogen as an internal gas chromatography (GC) standard, for a total flow of 110 sccm. The pressure of the system was maintained at 265 psig with a digital back-pressure regulator (Alicat), and the temperature was controlled across three zones of the reactor heated to 300 °C with 1 ft lengths of heating tape (Amptek) using K-type thermocouples and proportional–integral–derivative (PID) temperature controllers (Omega). Liquid products were collected in a high-pressure reactor vessel (Parr) cooled to 5 °C with an immersion cooler (SP Scientific) in a water bath, and the product gas stream was first dried over a bed of 3 Å molecular sieves prior to GC analysis (Agilent Technologies). Each experimental sequence was set for a total of 5 GC sampling runs with 12 h post-run intermission.

2.5. Ethylene Oligomerization. A fixed-bed reactor was prepared by loading a stainless-steel tube (9 in. length, $^1/_2$ in. outer diameter, and $^3/_8$ in. inner diameter) with variable amounts of either commercial or particle-formed Ni-exchanged ASA with commercial ASA filler (~10 g total). The catalyst was dried with flowing nitrogen at 300 °C overnight prior to introducing compressed ethylene at a flow rate (10 sccm) controlled by a mass flow controller (Sierra Instruments), where the temperature was established at 120 °C across three zones using K-type thermocouples and PID controllers (Omega). Liquid products were trapped in a 500 mL sample storage cylinder (Swagelok) chilled in an acetone bath to −50 °C with an immersion cooler (SP Scientific), and the pressure of the system was maintained with a digital back-pressure regulator to 415 psig. Liquid products were analyzed by gas chromatography–mass spectrometry (GC–MS, Agilent Technologies).

3. RESULTS AND DISCUSSION

3.1. Carbon Dioxide Hydrogenation. A catalyst formulation that has been previously well-characterized in a continuously stirred-tank reactor (CSTR) environment was used as the baseline catalyst to demonstrate the feasibility of using a silica-stabilized coating to enhance catalyst activity in a fixed-bed tubular reactor.[9,21] In the initial studies, the baseline catalyst was reduced in the fixed-bed tubular reactor by carbon monoxide to form iron carbide phases on the catalyst. It has been proposed that these carbide phases are essential in FT synthesis for chain growth.[32−34] This has been shown by changing the reducing agent of the fresh catalyst from CO to H_2, resulting in a lower CO conversion.[35] Table 1 provides the observed hydrogenation performance as CO_2 percent conversion and product distribution (CO and hydrocarbons) of the baseline catalyst reduced in CO. The reaction was run for over

dx.doi.org/10.1021/ef4011115 | Energy Fuels 2013, 27, 6348–6354

Table 3. Product Selectivity (%, Carbon Based), Olefin/Paraffin Ratio, CO_2 Conversion, and ASF Values over K/Mn/Fe Catalysts Impregnated on Al_2O_3 and Reduced in H_2 under Fixed-Bed Conditions

		selectivity (%, carbon based)										
time (h)	CO_2conversion (%)	CO (%)	C_1 (%)	C_2 (%)	C_3 (%)	C_4 (%)	C_5 (%)	C_6 (%)	C_2−C_{6+}	C_2−C_{6+} yield (%)	olefin/paraffin	α C_1−C_{6+}
12	38.1	14.1	34.1	16.8	18.9	13.1	3.0	0	51.8	19.7	4.4	0.22
24	33.8	14.8	28.0	15.0	17.4	12.9	10.0	1.9	57.2	19.3	5.1	0.44
36	33.9	13.5	26.2	14.8	16.8	11.8	8.9	8.0	60.3	20.4	5.2	0.54
48	33.2	13.0	24.7	14.4	16.7	12.0	9.2	10.0	62.9	20.9	5.3	0.57
60	33.7	12.2	24.7	14.7	16.9	11.8	9.0	10.6	63.0	21.2	5.4	0.57
72	33.4	11.9	23.8	14.4	16.7	11.9	9.3	12.1	64.4	21.5	5.5	0.58
90	34.7	11.4	24.6	14.8	17.1	11.8	8.5	11.8	64.0	22.2	5.4	0.57

Table 4. Product Selectivity (%, Carbon Based), Olefin/Paraffin Ratio, CO_2 Conversion, and ASF Values over K/Mn/Fe Catalysts Impregnated on Al_2O_3 and Reduced in H_2 under Fixed-Bed Conditions: Modified with TEOS

		selectivity (%, carbon based)										
time (h)	CO_2 conversion (%)	CO (%)	C_1 (%)	C_2 (%)	C_3 (%)	C_4 (%)	C_5 (%)	C_6 (%)	C_2−C_{6+}	C_2−C_{6+} yield (%)	olefin/paraffin	α C_1−C_{6+}
12	31.2	11.0	27.6	16.0	20.0	15.6	9.0	0.8	61.4	19.1	3.6	0.39
24	27.2	13.6	25.6	14.3	16.9	12.6	10.5	6.5	60.8	16.5	4.6	0.54
36	27.4	13.7	25.9	14.2	16.3	11.6	9.0	9.4	60.5	16.6	4.5	0.56
48	25.8	14.9	25.4	13.9	15.7	11.2	8.8	10.0	59.6	15.4	4.5	0.56
60	27.0	14.4	25.8	13.9	15.5	10.8	8.2	11.4	59.8	16.1	4.4	0.57
72	26.5	15.2	25.9	13.8	15.2	10.4	7.7	11.7	58.8	15.6	4.3	0.57
96	26.5	15.3	26.1	13.9	15.2	10.3	7.7	11.4	58.5	15.5	4.3	0.56
114	27.3	15.5	26.8	14.1	15.3	10.1	7.4	10.8	57.7	15.7	4.2	0.55

116 h. After the first 12 h, CO_2 conversion remained steady between 31 and 35%. The hydrocarbon selectivity (not including methane) increased to as high as 65.4% of the CO_2 converted, where the olefin/paraffin ratio remained stable at 5.3. A shift toward higher hydrocarbon selectivity was observed as the C_{6+} fraction increased from 0 to 9.0% over the course of 116 h. This is in agreement with pretreatment studies of Fe-based FT synthesis catalysts that showed that CO reduction led to longer hydrocarbon chains and less methane production.[36] Higher activities were also achieved after a slower approach (e.g., 50 h) to reach steady-state conditions.[37] Such an increase in activity is suspected to be a result of the increased basicity of the carbide phase at the catalyst surface, enhancing the absorption and dissociation of CO while also decreasing the frequency of secondary hydration reactions for olefin products.[38] Approximately 2.4 mL of liquid hydrocarbon were collected in the trap after 116 h.

Preliminary studies of the iron catalyst modified with 9% TEOS and tested for 8 h found that CO_2 conversion increased by as much as 22%.[21] In addition, the selectivity toward CO and methane was shown to decrease. When 9% TEOS was added to the baseline catalyst used in the present studies, Table 2 shows an 8.8% average decrease in overall CO_2 conversion after 12 h, as compared to the baseline catalyst. During this time, the CO selectivity increased by as much as 31% and methane selectivity increased very little. The loss in CO_2 conversion and the higher selectivity of CO reduced the overall hydrocarbon selectivity in the C_2−C_{6+} fraction. In addition, the selectivity within the C_2−C_{6+} fraction shifted away from the formation of olefins, as shown by a 30% decrease in the olefin/paraffin ratio over time.

Preliminary studies by Song et al.[21] report increases in CO_2 conversions by as much as 22% when H_2 was used as the reducing agent. The studies reported here include a comparison of CO to H_2 to elicit the role of the reducing agent on CO_2 conversion and hydrocarbon selectivity of the baseline catalyst and the modified catalyst. Table 3 provides the results of the baseline catalyst reduced in H_2. Comparing the baseline catalysts over time (Tables 1 and 3) shows that the CO_2 conversion is not notably affected by the reducing agent. While CO selectivity increases by about 12% over the baseline catalyst reduced in H_2, the hydrocarbon selectivity and the olefin paraffin ratios remain similar for both baseline catalysts. In addition, Table 3 shows a 32% shift in hydrocarbon selectivity toward C_{6+} over time. Indeed, 3.3 mL of liquid hydrocarbon was collected from the trap after 92 h compared to 2.4 mL collected after 116 h.

Table 4 provides the data collected for the modified catalyst reduced in H_2. Comparing the baseline catalyst and the modified catalyst reduced in H_2 (Tables 3 and 4) shows that the CO_2 conversion was reduced after the first 12 h by an average of 21% overtime and the methane selectivity increased by an average of 13% for the modified catalyst. A shift toward the formation of more saturated hydrocarbons is observed over the modified catalyst because the average olefin/paraffin ratio after the first 12 h is 4.4 compared to 5.3 for the baseline catalyst. In addition, the overall selectivity of C_2−C_{6+} is reduced on average 24% by the modification of the catalyst.

Comparing the modified catalyst reduced in CO and H_2 (Tables 2 and 4) shows that the modified catalyst reduced in H_2 has much greater selectivity toward olefins than the modified catalyst reduced in CO. It also produces 10% less CO over time. However, the modified catalyst in H_2 has the lowest average CO_2 conversion over time compared to the other catalyst and conditions.

In Tables 1−4, the yield is calculated by multiplying the C_2−C_{6+} hydrocarbon selectivity values with the CO_2 conversion values. Tables 1 and 3 show that, on average after 12 h, the C_2−C_{6+} yield is 21% on a carbon basis. This means that an average of 21% of CO_2 fed into the reactor is converted to C_2−C_{6+} molecules. This average yield of 21% for both baseline catalysts is significantly higher than the 17 and 16% yields obtain for the

dx.doi.org/10.1021/ef4011115 | Energy Fuels 2013, 27, 6348−6354

modified catalysts. Clearly, the addition of TEOS to the catalysts negatively affects the transport of species to the catalyst sites.

The total hydrocarbon product distribution as a function of time and catalyst modification can be described by means of Anderson–Schulz–Flory (ASF) growth distribution plots, where $\ln(W_N/N)$ (W_N is the weight fraction of HC containing N number of carbon atoms) is plotted as a function of the carbon number (N). The chain growth probability α is inferred by the slope.[39] Tables 1–4 show that, on average, the chain-growth probability for each catalyst condition reaches its maximum after 60 h. Tables 1 and 4 show that, while the average CO_2 conversion was reduced by the addition of TEOS to the baseline catalyst, the average chain-growth probability after 12 h increased slightly from 0.48 to 0.52 when the catalyst was reduced by CO. When the baseline catalyst was reduced in H_2 compared to reduction by CO, the average chain-growth probability increased from 0.48 to 0.54. This appears to be the result of a shift in hydrocarbon selectivity toward C_{6+} from an average of 6% (Table 1, catalyst reduced by CO) to 9% (Table 3, catalyst reduced by H_2). The average higher chain-growth probability for catalyst reduced by H_2 was not affected by the modification of the catalyst with TEOS. The tables indicate that, under the fixed-bed reaction conditions for CO_2 hydrogenation, reduction with CO is favored for the production of light ($<C_6$) olefins.

3.2. Ethylene Oligomerization: Catalyst Characterizaton. ASAs offer a robust catalyst platform that may be systematically tailored by controlling pore size distribution,[40−42] degree of crystallinity,[43] and number and strength of Brønsted and Lewis acidic sites[44] to optimize catalytic performance. Specifically, these catalysts are notably effective in oligomerization of propylene and butylene. Although previously reported results have established a foundation from which to approach the use of ASA supports for catalysis, there remains a challenge in tuning their properties to achieve specific hydrocarbon selectivity, such as 1-hexene, or a particular hydrocarbon region, such as C_9–C_{16}.

In this study, hydrogels were synthesized by co-precipitating aluminum and silica. By systematically altering the synthesis as a function of the aluminum content and pH, a set of support materials were generated (Table 5). The ASA supports were formed into particles by heating the gel to 110 °C within molds of a specified size, and nickel was loaded onto the resultant pelletized materials by ion exchange.[45] The catalysts were initially characterized by XPS, FTIR, BET, and elemental analysis to identify changes in ASA composition as a function of the proportion of used Si and Al precursors, pH of hydrogel isolation, nickel cation exchange, and calcination conditions. The synthesized ASA and NiASA particle characterization data are provided in Figure 2, where it was observed that the SiO_2/Al_2O_3 ratio increased with pH during hydrogel formation for 5% Al-containing ASA and less notably for the 15% Al-containing ASA. The observed higher Al surface concentration for calcinated samples is also supported by the expected increase in the SiO_2/Al_2O_3 ratio for calcinated samples reported in the literature.[46]

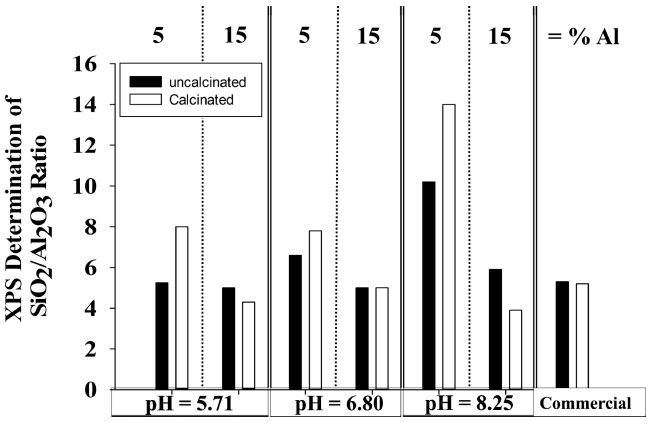

Figure 2. Ratio of SiO_2/Al_2O_3 as determined by XPS analysis for synthesized and commercial ASA of varying Al content (5 versus 15%) and uncalcinated (black bars) versus calcinated (white bars) samples.

Table 5. Properties of Synthesized ASA Materials Varying in Al Content (5 versus 15%)

sample	Al content (wt %)	synthesis (pH)	calcination	BET surface area (m^2/g)	Ni (atomic %)
1	5	5.71	uncalcinated	577	1.90
2	5	5.71	calcinated	373	0.41
3	5	6.80	uncalcinated	693	2.36
4	5	6.80	calcinated	471	0.54
5	5	8.25	uncalcinated	602	1.97
6	5	8.25	calcinated	346	0.43
7	15	5.71	uncalcinated	290	3.26
8	15	5.71	calcinated	116	0.19
9	15	6.80	uncalcinated	345	0.86
10	15	6.80	calcinated	248	0.47
11	15	8.25	uncalcinated	359	2.37
12	15	8.25	calcinated	227	0.20

With regards to Ni loading, elemental analysis indicates that there was a decreased Ni concentration for calcinated ASA when compared to uncalcinated ASA (Table 5). This was likely due to the depletion of surface silanol groups by dehydration that may be essential for Ni coordination.[47] Also, it was found that, in general, ASA with a higher Al content contained higher concentrations of Ni. Because it has been suggested that Al–OH–Si bridging hydroxyl groups are Ni-exchangeable sites in ASA-supported Ni catalysts,[36,48] it followed that an increase in the Al content would result in higher Ni loading. Indeed, the FTIR spectra of the Ni-loaded ASAs were identical to those of their Ni-free precursors, with the exception of a diminishing intensity in the broad silanol stretch at 3450 cm^{-1}. We did not identify any particular trends in the degree to which the silanol band had diminished and the conditions under which the ASA support materials were originally synthesized. However, we did generally find that the degree to which the silanol band diminished was less for the calcinated ASAs than for non-calcinated ASAs. This qualitatively indicates that the calcinated ASAs are less capable of loading Ni, probably because of a lower concentration of surface silanols. This hypothesis was supported by elemental analysis. Additionally, the calcinated ASAs were determined to have over a 30% loss in surface area by BET.

3.3. Ethylene Oligomerization: Catalyst Performance. In this study, pure ethylene was used as a model to test the optimization of well-characterized ASA-supported nickel catalysts for the selective oligomerization of olefins to higher molecular weight hydrocarbons in the C_9–C_{16} region. The ASA characterization shown in Table 5 verified that the uncalcinated

dx.doi.org/10.1021/ef4011115 | Energy Fuels 2013, 27, 6348–6354

supports contained higher nickel loading and greater surface area. In this evaluation, 20 g of uncalcinated, nickel-loaded ASA support synthesized using 5% Al at pH 5.71 (sample 1 in Table 5) was explored at different mass hourly space velocities (MHSVs) to determine conditions needed to achieve high ethylene conversion as well as ideal product selectivity (C_9−C_{16} olefins for fuel application). Figure 3 shows ethylene conversion

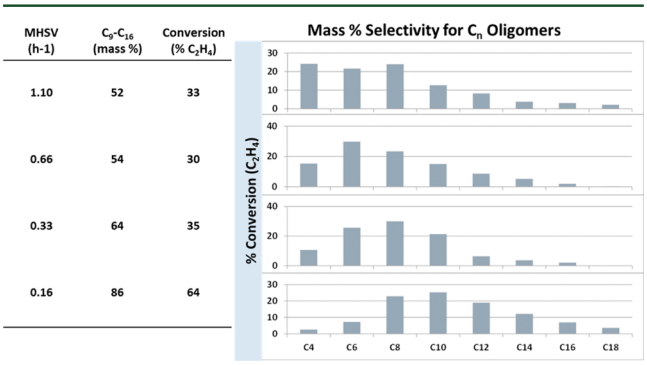

Figure 3. Performance of NiASA (5% Al, pH 5.71, and uncalcinated) with respect to changing percent conversion of ethylene and mass percent selectivity for chain number with the change in MHSV [flow rate (ethylene), 100 sccm; *P*, 415 psig; and *T*, 120 °C].

and the mass percent selectivity for hydrocarbon chain length as a function of the MHSV at 415 psig. The figure shows that, as MHSV was decreased from 1.10 to 0.16 h^{-1}, ethylene conversion increased from 33 to 64%. The remaining 67−36% of the ethylene was not converted. In addition, the hydrocarbon fraction detected in the C_9−C_{16} region increased from 52 to 86%. This observation was supported by literature reports, where increasing the retention time of reactant ethylene feed on the catalyst bed resulted in a lower MHSV value, allowing for further chain growth of the formed oligomer.[49]

4. CONCLUSION

The separate steps of CO_2 hydrogenation and ethylene oligomerization were explored to identify and improve catalyst composition and reaction conditions ideal for scale-up considerations. Initial results for CO_2 hydrogenation demonstrated a loss in conversion and hydrocarbon selectivity to olefins by the modification of a Fe/Mn/K catalyst supported on alumina with TEOS under fixed-bed conditions. Further, the results indicated that, under fixed-bed reaction conditions for CO_2 hydrogenation, the Fe/Mn/K catalyst produced lighter olefins in greater quantities when CO was used as the reducing agent.

Characterization of ASA formed under conditions of different Al content, pH of synthesis, and calcination treatment indicated that the structure of ASA supports can be directed to control Ni catalyst loading as well as the surface silica/alumina ratio. Preliminary tests indicated that the formed NiASA performed well as a catalyst for the oligomerization of ethylene, where ethylene conversion as well as selectivity for oligomers of higher chain length were successfully targeted by decreasing the MHSV. As such, the pelletized NiASA is considered as a potential catalyst for the upgrading of light olefins from an initial CO_2 hydrogenation reactor to higher olefins of jet fuel-specific composition when used in either a merged or separated oligomerization stage reactor. These results indicate promising directions for conditions and catalyst compositions to use in the scale-up demonstration of CO_2-to-fuel conversion, where there is ongoing work to improve reactor design, catalyst compositions, and reaction and process conditions (e.g., CO_2 hydrogenation in a single step to liquid olefins).

AUTHOR INFORMATION

Corresponding Author

*Telephone: +01-202-767-2673. E-mail: heather.willauer@nrl.navy.mil.

Notes

The authors declare no competing financial interest.

ACKNOWLEDGMENTS

This work was supported by the Office of Naval Research both directly and through the NRL.

REFERENCES

(1) Olah, G. A.; Goeppert, A.; Prakash, G. K. S. *Beyond Oil and Gas: The Methanol Economy*; Wiley-VCH Verlag GmbH and Co.: Weinheim, Germany, 2006.
(2) Coffey, T.; Hardy, D. R.; Besenbruch, G. E.; Schultz, K. R.; Brown, L. C.; Dahlburg, J. P. *Def. Horiz.* **2003**, *36*, 1.
(3) Willauer, H. D.; Hardy, D. R.; Lewis, M. K.; Ndubizu, E. C.; Williams, F. W. *Energy Fuels* **2009**, *23*, 1770−1774.
(4) Willauer, H. D.; Hardy, D. R.; Lewis, M. K.; Ndubizu, E. C.; Williams, F. W. *J. Phys. Chem. A* **2010**, *114*, 4003−4008.
(5) Willauer, H. D.; Hardy, D. R.; Lewis, M. K.; Ndubizu, E. C.; Williams, F. W. *Energy Fuels* **2010**, *24*, 6682−6688.
(6) Willauer, H. D.; DiMascio, F.; Hardy, D. R.; Lewis, M. K.; Williams, F. W. *Ind. Eng. Chem. Res.* **2011**, *50*, 9876−9882.
(7) Dorner, R. W.; Hardy, D. R.; Williams, F. W.; Davis, B. H.; Willauer, H. D. *Energy Fuels* **2009**, *23*, 4190−4195.
(8) Dorner, R. W.; Hardy, D. R.; Williams, F. W.; Willauer, H. D. *Catal. Commun.* **2010**, *11*, 816−819.
(9) Dorner, R. W.; Hardy, D. R.; Williams, F. W.; Willauer, H. D. *Appl. Catal., A* **2010**, *373*, 112−121.
(10) Dorner, R. W.; Hardy, D. R.; Williams, F. W.; Willauer, H. D. *Catal. Commun.* **2011**, *15*, 88−99.
(11) Riedel, T.; Schaub, G.; Jun, K.-W.; Lee, K.-W. *Ind. Eng. Chem. Res.* **2001**, *40*, 1355−1363.
(12) Ning, W.; Koizumi, N.; Yamada, M. *Energy Fuels* **2009**, *23*, 4696−4700.
(13) Pan, Y.-X.; Liu, C.-J.; Ge, Q. *J. Catal.* **2010**, *272*, 227−234.
(14) Dorner, R. W.; Hardy, D. R.; Williams, F. W.; Willauer, H. D. *Energy Environ. Sci.* **2010**, *3*, 884−890.
(15) Wang, W.; Wang, S.; Ma, X.; Gong, J. *Chem. Soc. Rev.* **2011**, *40*, 3703−3727.
(16) Centi, G.; Iaquaniello, G.; Perathoner, S. *ChemSusChem* **2011**, *4*, 1265−1273.
(17) Quadrelli, E. A.; Centi, G.; Duplan, J. L.; Perathoner, S. *ChemSusChem* **2011**, *4*, 1194−1215.
(18) Wu, J.; Saito, M.; Takeuchi, M.; Watanabe, T. *Appl. Catal., A* **2001**, *218*, 235−240.
(19) Botes, F. G. *Catal. Rev.* **2008**, *50*, 471−491.
(20) Baya, M.; Rahimpour, M. R. *J. Nat. Gas Sci. Eng.* **2012**, *9*, 73−85.
(21) Ding, F.; Zheng, B.; Song, C.; Guo, X. *Prep. Pap.—Am. Chem. Soc., Div. Fuel Chem.* **2012**, *57*, 444.
(22) Jarallah, A. M. A. *J. Catal.* **1992**, *14*, 1−124.
(23) Olah, G. A.; Molinár, A. Oligomerization and polymerization. In *Hydrocarbon Chemistry*, 2nd ed.; John Wiley and Sons, Inc.: Hoboken, NJ, 2003; pp 723−806.
(24) de Klerk, A. *Energy Fuels* **2006**, *20*, 1799−1805.
(25) Heveling, J.; Nicolaides, C. P.; Scurrell, M. S. *Appl. Catal., A* **1998**, *173*, 1−9.
(26) Heveling, J.; Nicolaides, C. P.; Scurrell, M. S. *Catal. Lett.* **2004**, *95*, 87−91.
(27) Heveling, J.; Nicolaides, C. P. *Catal. Lett.* **2006**, *107*, 117−121.

(28) Heydenrych, M. D.; Nicolaides, C. P.; Scurrell, M. S. *J. Catal.* **2001**, *197*, 49−57.
(29) Lallemand, M.; Finiels, A.; Fajula, F.; Hulea, V. *J. Phys. Chem. C* **2009**, *113*, 20360−20364.
(30) Heveling, J.; Nicolaides, C. P.; Scurrell, M. S. *Chem. Commun.* **1991**, 126−127.
(31) Hensen, E. J. M.; Poduval, D. G.; Magusin, P. C. M. M.; Coumans, A. E.; van Veen, J. A. R. *J. Catal.* **2010**, *269*, 201−218.
(32) Shroff, M. D.; Kalakkad, D. S.; Coulter, K. E.; Kohler, S. D.; Harrington, M. S.; Jackson, N. B.; Sault, A. G.; Datye, A. K. *J. Catal.* **1995**, *156*, 185−207.
(33) Li, S. Z.; Krishnamoorthy, S.; Li, A. W.; Meitzner, G. D.; Iglesia, E. *J. Catal.* **2002**, *206*, 202−217.
(34) Herranz, T.; Rojas, S.; Perez-Alonso, F. J.; Ojeda, M.; Terreros, P.; Fierro, J. L. G. *J. Catal.* **2006**, *243*, 199−211.
(35) Bukur, D. B.; Nowicki, L.; Manne, R. K.; Lang, X. S. *J. Catal.* **1995**, *155*, 366−375.
(36) Bukur, D. B.; Nowicki, L.; Patel, S. A. *Can. J. Chem. Eng.* **1996**, *74*, 399−404.
(37) Bukur, D. B.; Lang, X.; Ding, Y. *Appl. Catal., A* **1999**, *186*, 255−275.
(38) Zhang, J.-L.; Ma, L.-H.; Fan, S.-B.; Zhao, T.-S.; Sun, Y.-H. *Fuel* **2013**, 116−123.
(39) Ma, W.-P.; Zhao, Y.-L.; Li, Y.-W.; Xu, Y.-Y.; Zhou, J.-L. *React. Kinet. Catal. Lett.* **1999**, *66*, 217−223.
(40) Snel, R. *Appl. Catal.* **1987**, *33*, 281−294.
(41) Carati, A.; Ferraris, G.; Guidotti, M.; Moretti, G.; Psaro, R.; Rizzo, C. *Catal. Today* **2003**, *77*, 315−323.
(42) Vít, Z.; Šolcová, O. *Microporous Mesoporous Mater.* **2006**, *96*, 197−204.
(43) Nicolaides, C. P. *Appl. Catal., A* **1999**, *185*, 211−217.
(44) Bartoszek, M.; Eckelt, R.; Jäger, C.; Kosslick, H.; Pawlik, A.; Schulz, A. *J. Mater. Sci.* **2009**, *44*, 6629−6636.
(45) Heveling, J.; Nicolaides, C. P.; Scurrell, M. S. *J. Chem. Soc., Chem. Commun.* **1991**, 126−127.
(46) Pieta, I. S.; Ishaq, M.; Wells, R. P. K.; Anderson, J. A. *Appl. Catal., A* **2010**, *390*, 127−134.
(47) Crepau, G.; Montillout, V.; Vjmont, A.; Ariey, L.; Cseri, T.; Maugé, F. *J. Phys. Chem. B* **2006**, *110*, 15172−15185.
(48) Burwell, R. L., Jr. *Chemtracts* **1991**, *July/August*, 242−244.
(49) de Klerk, A.; Engelbrecht, D. J.; Boikanyo, H. *Ind. Eng. Chem. Res.* **2004**, *43*, 7449−7455.